

Time-Optimal Coherence-Order-Selective Transfer of In-Phase Coherence in Heteronuclear I/S Spin Systems

Timo O. Reiss,* Navin Khaneja,† and Steffen J. Glaser*¹

**Institut für Organische Chemie und Biochemie II, Technische Universität München, Lichtenbergstrasse 4, 85747 Garching, Germany;*
and †*Division of Applied Sciences, Harvard University, Cambridge, Massachusetts 02138*

E-mail: timo.reiss@ch.tum.de, navin@hrl.harvard.edu, glaser@ch.tum.de

Received April 16, 2001; published online January 16, 2002

Based on principles of geometric optimal control theory, coherence transfer building blocks can be derived which achieve optimal sensitivity. Here, experimental pulse sequences are presented that achieve the best possible coherence-order-selective in-phase transfer ($S^- \rightarrow I^-$) for a heteronuclear 2-spin system for any given mixing time in the absence of relaxation. For short mixing times, the optimal experiment improves the sensitivity of isotropic mixing by up to 12.5%. © 2002 Elsevier Science (USA)

Key Words: optimal control theory; coherence transfer; isotropic mixing; sensitivity enhancement; TOCSY.

1. INTRODUCTION

In order to maximize the sensitivity of NMR experiments, optimal pulse sequence elements are desirable for each individual coherence transfer step (I). If relaxation can be neglected, theoretical upper bounds can be derived for the transfer between arbitrary initial and final terms of the density operator (2–4). In practice, it is desirable to reach these bounds as fast as possible in order to reduce relaxation losses during the transfer period (5). For applications to biomolecules, relaxation rates are often comparable or even larger than typical coupling constants. A commonly used approach to take relaxation losses into account is to reduce the mixing time τ_{mix} of experimental building blocks that reach the unitary bound in the absence of relaxation, in order to find a compromise between coherence transfer and relaxation losses. However, as discussed below, this approach leads in general to suboptimal solutions. Theoretical and practical issues related to this problem are:

1. What is the shortest mixing time τ_{mix}^* for which the unitary bound (3, 4) of a desired transfer can be reached in a given spin system?
2. What is the maximum transfer amplitude (in the absence of relaxation) for mixing times $\tau_{mix} < \tau_{mix}^*$ and what are the corresponding unitary transformations?

3. Which experimental building blocks implement the optimal unitary transformations for $\tau_{mix} < \tau_{mix}^*$?

In a recent theoretical paper (6), the first and second issues were solved analytically for coherence-order-selective coherence transfer (4) in heteronuclear I/S spin systems. In this paper, these theoretical results are translated into practical pulse sequences and the theoretical predictions are tested experimentally. This demonstrates that the commonly used strategy for the adjustment of pulse sequence elements in the presence of relaxation can give suboptimal results: In general, it is not sufficient to simply reduce the mixing period of a given transfer step in order to find a compromise between coherence transfer and relaxation losses. In addition, it can be necessary to modify the pulse sequence in order to achieve maximum transfer efficiency.

2. THEORY

We consider a heteronuclear I/S spin system with offsets ν_I and ν_S and a scalar coupling constant J . The corresponding Hamiltonian \mathcal{H} has the form

$$\mathcal{H}_0 = 2\pi \nu_I I_z + 2\pi \nu_S S_z + 2\pi J I_z S_z. \quad [1]$$

For coherence-order-selective transfer of in-phase coherence from spin S to spin I , the initial density operator is $\rho(0) = S^- = S_x - iS_y$ and the target operator is $I^- = I_x - iI_y$. The normalized absolute value of the transfer amplitude for a given mixing period τ_{mix} is given by (4)

$$\eta(\tau_{mix}) = \frac{| \langle I^- | \rho(\tau_{mix}) \rangle |}{\|S^-\| \|I^-\|} = \frac{1}{2} \text{Tr}\{I^+ \rho(\tau_{mix})\}. \quad [2]$$

Our goal is to find optimal pulse sequences that maximize the transfer amplitude $\eta(\tau)$ for any given mixing period τ . Based on principles of geometric optimal control theory (7), it has been shown recently (6) that the optimal mixing Hamiltonian \mathcal{H}_{mix}

¹ To whom correspondence should be addressed. Fax: ++49 (0)89 289-13210.

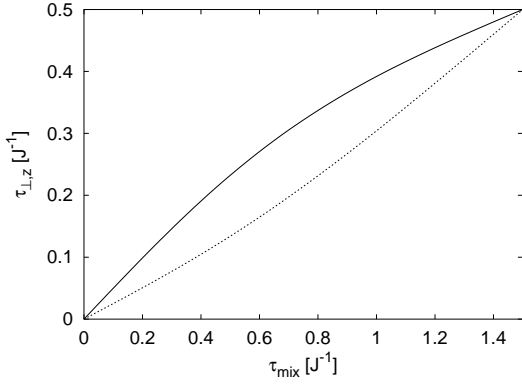


FIG. 1. Graphical representation of the optimal mixing times τ_z (solid line) and $\tau_{\perp} = \tau_x = \tau_y$ (dashed line) as a function of the overall mixing time τ_{mix} .

depends on the duration τ of the mixing period and has the general form

$$\mathcal{H}_{opt} = \frac{2\pi J}{\tau_{mix}} (\tau_x I_x S_x + \tau_y I_y S_y + \tau_z I_z S_z) \quad [3]$$

with

$$\tau_{mix} = \tau_x + \tau_y + \tau_z \quad [4]$$

and

$$\tau_x = \tau_y = \tau_{\perp} = \frac{1}{J\pi} \arctan\left(\frac{1}{2} \tan(J\pi\tau_z)\right) \quad [5]$$

(see Fig. 1). For any given mixing time $\tau_{mix} < 1.5J^{-1}$, the corresponding optimum transfer efficiency $\eta_{opt}(\tau_{mix})$ is given by

$$\eta_{opt}(\tau_{mix}) = \sin(J\pi\tau_z) \sin(J\pi\tau_{\perp}) \quad [6]$$

(see solid line in Fig. 2). For $\tau_{mix} \geq 1.5J^{-1}$ the transfer efficiency $\eta_{opt}(\tau_{mix})$ is 1, which corresponds to the unitary bound for this transfer (4). Hence, the minimum time that is required to reach the unitary bound is given by

$$\tau_{mix}^* = 1.5J^{-1}. \quad [7]$$

According to Eqs. [3]–[5] and Fig. 1, \mathcal{H}_{opt} approaches the isotropic mixing Hamiltonian (8–10) with $\tau_x = \tau_y = \tau_z = \tau_{mix}/3$ for the mixing time $\tau_{mix} = \tau_{mix}^*$. This corresponds to the well-known fact that isotropic mixing reaches the unitary bound at $\tau_{mix} = 1.5J^{-1}$ (10) and makes it interesting to compare the optimal transfer efficiency $\eta_{opt}(\tau_{mix})$ (Eq. [6]) with the transfer efficiency

$$\eta_{iso}(\tau_{mix}) = \sin^2(\pi J \tau_{mix}/3) \quad [8]$$

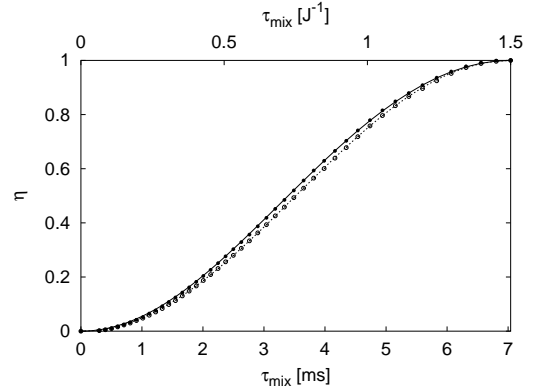


FIG. 2. Transfer amplitude of the optimal transfer η_{opt} (theoretical curve, see Eq. [6], solid line; experimental data; filled circles) as a function of the mixing time τ_{mix} for a coupling constant of 213 Hz. In addition, the transfer amplitude of isotropic mixing η_{iso} (theoretical curve, see Eq. [8], dashed line; experimental data; open circles) is also shown.

of heteronuclear isotropic mixing experiments (10) (see dashed line in Fig. 2).

In Fig. 2, the curves $\eta_{opt}(\tau_{mix})$ and $\eta_{iso}(\tau_{mix})$ are plotted and the ratio of these two curves is shown in Fig. 3. In the limit of short mixing times $\tau_{mix} \ll \tau_{mix}^*$, the transfer amplitude of the optimal mixing Hamiltonian is up to 12.5% larger compared to conventional isotropic mixing (cf. Fig. 3).

Assuming for simplicity that relaxation results in a simple exponential decay of coherences with an overall relaxation rate Γ , the maxima of the damped functions $\eta_{opt}(\tau_{mix}) \times \exp\{-\Gamma\tau_{mix}\}$ and $\eta_{iso}(\tau_{mix}) \times \exp\{-\Gamma\tau_{mix}\}$ can be determined. The ratio of these maxima is plotted in Fig. 4 as a function of the relaxation rate Γ for $0 \leq \Gamma \leq 7J$. For relaxation rates that are on the order of $2J$, the maximum transfer amplitude of the optimal mixing Hamiltonian is about 6% larger than that for isotropic mixing and for $\Gamma > 5J$ the gain exceeds 10%.

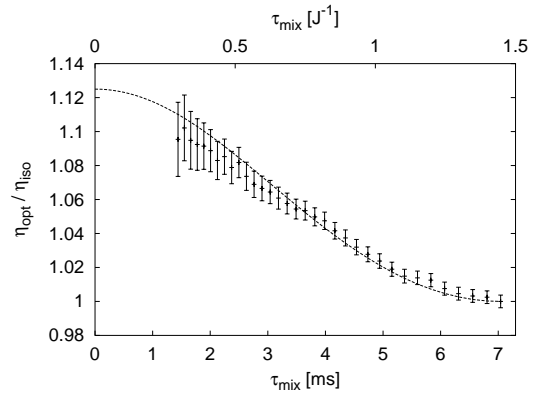


FIG. 3. Theoretical (dashed curve) and experimental ratio η_{opt}/η_{iso} of the transfer amplitudes of optimal and isotropic mixing experiments for coherence-order-selective in-phase transfer as a function of the mixing period τ_{mix} .

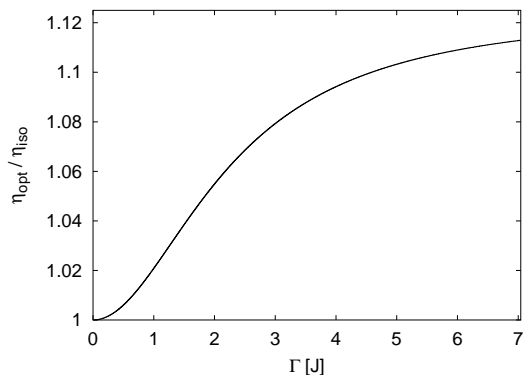


FIG. 4. Gain of the optimal mixing Hamiltonian compared to isotropic mixing as a function of the relaxation rate Γ (in units of the scalar coupling constant J).

3. EXPERIMENTS

In order to test the theoretical predictions, the optimal mixing Hamiltonian \mathcal{H}_{opt} and the isotropic mixing Hamiltonian \mathcal{H}_{iso} were implemented using the ^{13}CH moiety of chloroform (70% CHCl_3 dissolved in acetone- d_6 , $T = 25^\circ\text{C}$) as a model IS spin system with a coupling constant $J = 213$ Hz. Figure 5 shows the pulse sequence used to acquire experimental transfer functions. In-phase S spin (^{13}C) coherence (S_x) was prepared using heteronuclear NOE followed by a $90_y^\circ(S)$ pulse. Spoil gradients were applied prior to the initial $90_y^\circ(S)$ pulse and heteronuclear coherence transfer echoes ($I1$, $I2$) were created by gradients in order to select coherence-order-selective in-phase transfer (5) and to suppress the $^{12}\text{CHCl}_3$ signal. During detection of the spin I signal, spin S was decoupled. In the transfer block (gray box in Fig. 5), various pulse sequence elements can be inserted in order to test their transfer efficiency.

Experimental building blocks to implement the optimal mixing Hamiltonian \mathcal{H}_{opt} can be derived from well-known pulse sequence elements ($I3$) by simply adjusting the delays τ_x , τ_y , and τ_z according to Eq. [5]. We used the zyx -ICOS-CT sequence (cf. Fig. 5a) ($I3$) as a basis for the optimal and isotropic mixing experiments. Note that even for $\tau_x = \tau_y = \tau_z$, this sequence would only represent a true isotropic mixing Hamiltonian if at the end an additional $90_x^\circ(S)$ pulse would be applied, followed by a $90_z^\circ(I, S)$ rotation. However, for the transfer of S^- (or S^+) to I^- , the additional pulses and rotations have no effect on the transfer efficiency and can be omitted. In order to reduce the effects of experimental imperfections such as rf inhomogeneity, we further minimized the number of pulses for our experimental test: In the IS model system, the offsets of both spins can be set to zero (i.e., $\nu_I = \nu_S = 0$ Hz) which eliminates the need for the six 180° pulses which only serve to refocus the effect of the offset terms in \mathcal{H}_0 . However, as an odd number of 180° pulses is removed for each spin I and S , the coherence order of the transfer is reversed; i.e., the modified sequence in Fig. 5b effects the

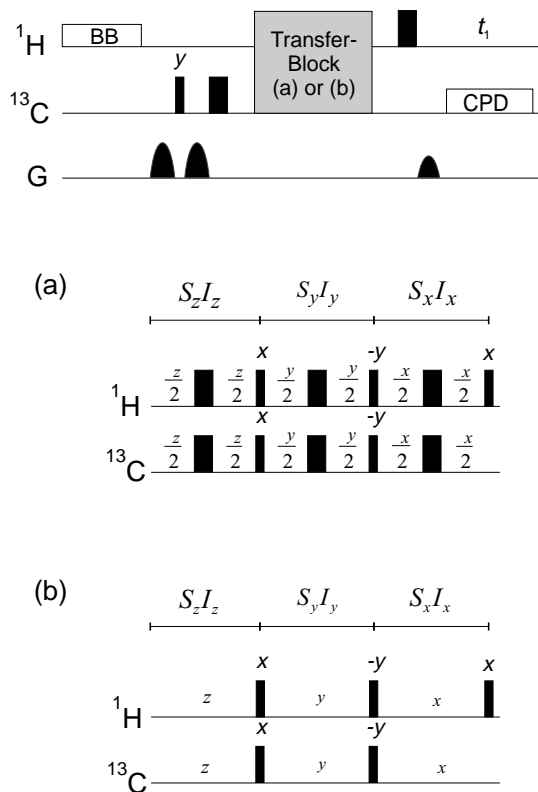


FIG. 5. Optimal pulse sequence elements for coherence-order-selective in-phase transfer: (a) zyx -ICOS-CT sequence ($I3$) and (b) simplified sequence for offsets $\nu_I = \nu_S = 0$ Hz. The delays τ_x , τ_y , and τ_z for the optimal transfer are given in Eq. [5]. An isotropic effective mixing Hamiltonian results for $\tau_x = \tau_y = \tau_z = \tau_{\text{mix}}/3$.

transfer S^\pm to I^\mp rather than S^\pm to I^\pm . In our experiments, this was taken into account by inverting the sign of the refocusing gradient prior to detection. Alternatively, the phase of the last $90^\circ(I)$ pulse could be inverted, in order to effect a transfer from S^\pm to I^\pm .

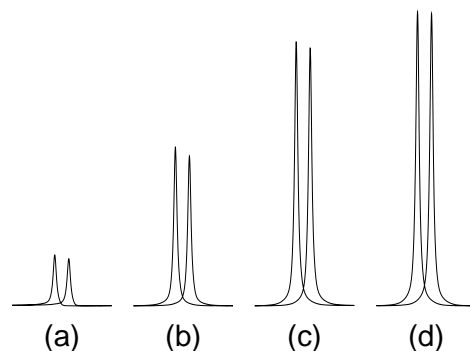


FIG. 6. ^1H spectra of $^{13}\text{CHCl}_3$ after optimal (left signal in each set) and isotropic (right signal in each set) coherence-order-selective coherence transfer from ^{13}C with mixing times τ_{mix}^* of (a) 1.76 ms = $0.267\tau_{\text{mix}}^*$, (b) 3.52 ms = $0.515\tau_{\text{mix}}^*$, (c) 5.28 ms = $0.788\tau_{\text{mix}}^*$, and (d) 7.04 ms = τ_{mix}^* .

For the optimal and the isotropic transfers, experimental spectra were recorded for 47 different mixing times $\tau_{mix} \leq \tau_{mix}^*$ with 42 scans each and a relaxation delay of 30 s. For mixing times $\tau_{mix} \approx (1/4)\tau_{mix}^*$, $\tau_{mix} \approx (1/2)\tau_{mix}^*$, $\tau_{mix} \approx (3/4)\tau_{mix}^*$, and $\tau_{mix} = \tau_{mix}^*$, sample spectra are shown in Fig. 6. In Fig. 2, integrated experimental signal amplitudes are shown (circles) and a good match between experimental and theoretical data is found. For a better comparison of the relative transfer amplitudes of optimal and isotropic transfer experiments, the ratio of the experimental transfer amplitudes is also plotted in Fig. 3. Again, a reasonably good match is found between theory and experiment. The small systematic deviation for short mixing times can be attributed to the incomplete suppression of the $^{12}\text{CHCl}_3$ signal; no attempt was made to correct for this residual artifact.

4. CONCLUSION

Based on the principles of geometric optimal control theory, the best possible coherence transfer amplitude can be derived for coherence transfer in spin systems consisting of two coupled spins (6). Compared to conventionally used experiments (isotropic mixing), gains of up to 12.5% were theoretically predicted for the transfer of S^- to I^- in an IS spin system. We have demonstrated that optimal transfer amplitudes can be realized experimentally by simply adjusting the parameters of existing pulse sequence elements. Even moderate gains in transfer efficiency can be significant in practical application, in particular if several such transfer steps are used in a given experiment. For example, the duration of an experiment with three consecutive coherence-order-selective in-phase transfer steps could be reduced by more than 25% (50%) without reducing the overall sensitivity, if the transfer amplitude of each transfer step could be improved by 5% (12.5%). The sequences presented were analyzed assuming that relaxation simply leads to an exponential overall damping function with a given relaxation rate Γ . However, this simplified view does not take into account the fact that for a given spin system some terms of the density operator relax more slowly than others and further sensitivity gains are expected by including concrete relaxation mechanisms in the optimization procedure.

ACKNOWLEDGMENTS

This work was supported by the DFG under Grant GI 203/4-1 and the Fonds der Chemischen Industrie.

REFERENCES

1. R. R. Ernst, G. Bodenhausen, and A. Wokaun, "Principles of Nuclear Magnetic Resonance in One and Two Dimensions," Clarendon Press, Oxford (1987).
2. O. W. Sørensen, Polarization transfer experiments in high-resolution NMR spectroscopy, *Prog. NMR Spectrosc.* **21**, 503–569 (1989).
3. O. W. Sørensen, A universal bound on spin dynamics, *J. Magn. Reson.* **86**, 435–440 (1990).
4. S. J. Glaser, T. Schulte-Herbrüggen, M. Sieveking, O. Schedletzy, N. C. Nielsen, O. W. Sørensen, and C. Griesinger, Unitary control in quantum ensembles, maximizing signal intensity in coherent spectroscopy, *Science* **208**, 421–424 (1998).
5. T. Untidt, T. Schulte-Herbrüggen, B. Luy, S. J. Glaser, C. Griesinger, O. W. Sørensen, and N. C. Nielsen, Design of NMR pulse experiments with optimum sensitivity: Coherence-order-selective transfer in I_2S and I_3S spin systems, *Mol. Phys.* **95**, 787–796 (1998).
6. N. Khaneja, R. W. Brockett, and S. J. Glaser, Time optimal control in spin systems, *Phys. Rev. A* **63**, 032308 (2001).
7. R. W. Brockett, System theory on group manifolds and coset spaces, *SIAM J. Control* **10**, 2 (1972).
8. D. P. Weitekamp, J. R. Garbow, and A. Pines, Determination of dipole coupling constants using heteronuclear multiple quantum NMR, *J. Chem. Phys.* **77**, 2870–2883 (1982); Erratum, *J. Chem. Phys.* **80**, 1372 (1984).
9. P. Caravatti, L. Braunschweiler, and R. R. Ernst, Heteronuclear correlation spectroscopy in rotating solids, *Chem. Phys. Lett.* **100**, 305–310 (1983).
10. S. J. Glaser and J. J. Quant, Homonuclear and heteronuclear Hartmann–Hahn transfer in isotropic liquids, in "Advances in Magnetic and Optical Resonance" (W. S. Warren, Ed.), Vol. 19, pp. 59–252, Academic Press, San Diego (1996).
11. A. A. Maudsley, A. Wokaun, and R. R. Ernst, Coherence transfer echoes, *Chem. Phys. Lett.* **55**, 9–14 (1978).
12. R. E. Hurd and B. K. John, Gradient-enhanced proton-detected heteronuclear multiple-quantum coherence spectroscopy, *J. Magn. Reson.* **91**, 648–653 (1991).
13. M. Sattler, P. Schmidt, J. Schleucher, O. Schedletzy, S. J. Glaser, and C. Griesinger, Novel pulse sequences with sensitivity enhancement for in-phase coherence transfer employing pulsed field gradients, *J. Magn. Reson. B* **108**, 235–242 (1995).